PERIODICA POLYTECHNICA SER. MECH. ENG. VOL. 50, NO. 1, PP. 63–72 (2006)

EXAMINATION OF THE TENSILE STATE OF FIBERS IN BRAIDED FIBER REINFORCED COMPOSITE TUBES

Balázs ZSIGMOND and László M. VAS

Department of Polymer Engineering
Budapest University of Technology and Economics
H–1521 Budapest, Hungary
Phone: 361/463-2003, Fax: 361/463-1527
e-mail: zsigmond@pt.bme.hu

Received: April 26, 2005

Abstract

Braided composite rods and tubes offer a special possibility of structures tailored to loading. In this paper the contraction in the cross-section of a braided carbon/epoxy-acrylate tube is modelled and tested during tensile test. For the model the reinforcing fibrous structure was assumed to be located on the middle surface of the tube both before and during deformation. A hyperbolic type function was derived for describing the cross-section which was measured by a videoextensometer. The theory gave a good agreement with the measurements before neck-forming.

Keywords: braiding, contraction, fiber reinforced composite.

Introduction

The appearance of high performance polymer composites has widened the variety of structural materials since they have opened a new perspective in the realization of engineering structures tailored to loading. Pre-designable anisotropy, the direction-dependence of mechanical properties, is the most advantageous characteristic of composite structures. Carbon fibers, for instance built in parallel to loading can increase the strength of the polyester structure by orders of magnitude, even to hundred fold of the original value.

Textile structures form not only a set of loose and independent fibers but are also interconnected systems of fiber bundles – such as a fabric prepared from carbon and glass fiber rovings – hence they provide further benefits as composite reinforcements.

In this paper the contraction of the braided composite tube is modelled during tensile loading which is important to know in order to model its mechanical behaviour.

1. Examination of the Tensile State of Fibers in Braided Fiber Reinforced Composite Tubes

Making use of the known geometrical and mechanical properties of the given fibers, a statistical single fiber model, which is perfectly flexible and elastic but breaks at a random value of load can be defined [1]–[7].

The tensile or shear test of the bundle induces the strain of the fibers. Assume that a tensile test is carried out on a fiber bundle, then the expression to calculate this strain ε of a fiber versus bundle strain u and bundle shear deformation w depends on the fiber position and is given by (see *Fig. 1*):

$$\varepsilon = \frac{l}{l_o} - 1 = (1+\varepsilon_o) \cdot \sqrt{\frac{(1+u)^2 + (T_o + w)^2}{1 + T_o^2}} - 1. \tag{1}$$

In *Eq.* (1) l_o, ε_o, e_o, $L_o = x_o$, l,$L = x$ are the unloaded length, the initial strain

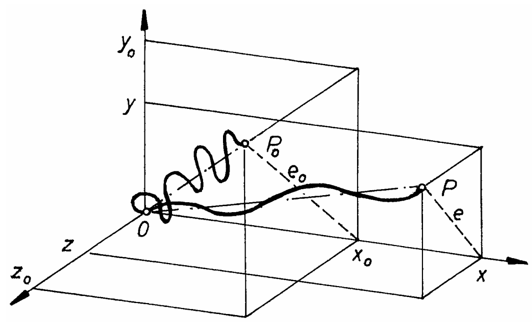

Fig. 1. The arrangement of a single fiber in a flat fiber bundle before and after loading [6]

before loading, and the initial excentricity or skewness of the fiber, of the initial and loaded lengths of the bundle, the loaded length of fiber after tensile and shear loads, respectively, as well as

$$u = \frac{\Delta L}{L_o} = \frac{L - L_o}{L_o}, \tag{2}$$

$$w = \frac{\Delta e}{L_o} = \frac{e - e_o}{L_o}, \tag{3}$$

$$e_o^2 = y_o^2 + z_o^2, \tag{4}$$

$$e^2 = y^2 + z^2, \tag{5}$$

$$T_o = \frac{e_o}{L_o}. \tag{6}$$

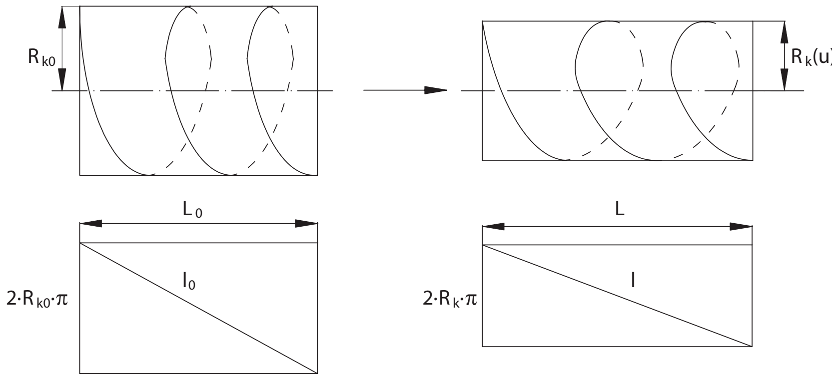

Fig. 2. Deformation of a tow in the middle surface of the braided composite

In the next examination the fibers will be considered linear elastic.

Suppose that the fibers are on the middle surface of the composite tube. There is a tensile stress in the fibers of the loaded composite if the elongation is positive, i.e. the loaded length (l) is higher than the unloaded one (l_0) (see the notations of *Fig*. 2: $l \geq l_0$):

$$\sqrt{4R_k^2 \cdot \pi^2 + L^2} = l \geq l_0 = \sqrt{4R_{k0}^2 \cdot \pi^2 + L_0^2}, \tag{7}$$

where L_0, R_{k0} and L, R_k are the unloaded and loaded length and middle radius of the composite, respectively. Let $L = L_0 \cdot (1 + u)$, where $u = \frac{\Delta L}{L_0}$ is the relative elongation of the composite. The following quantities are introduced

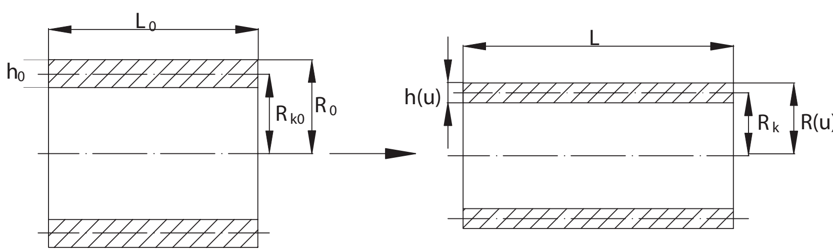

Fig. 3. Changing volume of a braided composite tube during loading

$$k_0 = \frac{R_{k0}}{L_0}, \tag{8}$$

$$\rho_k(u) = \frac{R_k(u)}{R_{k0}}, \tag{9}$$

$$k(u) = \frac{R_k(u)}{L_0} = \frac{R_{k0}}{L_0} \cdot \frac{R_k(u)}{R_{k0}} = k_0 \cdot \rho_k(u). \tag{10}$$

Eqs (8,9,10) are substituted into *Eq.* (1) and then it is squared and sorted:

$$\rho_k^2(u) \geq 1 - \frac{(1+u)^2 - 1}{4\pi^2 \cdot k_0^2}. \tag{11}$$

The condition of elongation above should be completed with the fact that the loaded middle radius ($R_k(u)$) is less then the original (R_{k0}):

$$1 \geq \rho_k(u) \geq \sqrt{1 - \frac{(1+u)^2 - 1}{4\pi^2 \cdot k_0^2}} = \rho_{kA}(u), \tag{12}$$

where $\rho_{kA}(u)$is the low boundary function.

External radii (R_0, $R(u)$) and thickness (h_0, $h(u)$) are used to determine the ratio of middle radii (*Fig. 1*), where R_0, $R(u)$ are the initial and loaded external radii, respectively:

$$\rho_k(u) = \frac{R(u) - \frac{h(u)}{2}}{R_0 - \frac{h_0}{2}}, \tag{13}$$

$$\text{introducing} : \Phi_0 = \frac{h_0}{R_0}, \text{hence} \tag{14}$$

$$\rho_k(u) = \frac{\frac{R(u)}{R_0} - \frac{\Phi_0}{2} \cdot \frac{h(u)}{h_0}}{1 - \frac{\Phi_0}{2}}, \tag{15}$$

$$\text{using additionally} : \delta(u) = \frac{h(u)}{h_0}, \tag{16}$$

on the other hand the external radii is described with *Eq.* (12)

$$\rho(u) = \frac{R(u)}{R_0} \geq \left(1 - \frac{\Phi_0}{2}\right) \cdot \rho_{kA}(u) + \frac{\Phi_0}{2} \cdot \delta(u) \tag{17}$$

It is to be noted that the right side of *Eq.* (17) is the convex linear combination of $\rho_{kA}(u)$ and $\delta(u)$ functions.

If the volume change is considered

In the case of the pure tensile loading of the continuum, the volume cannot decrease (using the notations of *Fig. 3*).

$$V \geq V_0 \tag{18}$$

$$\left(R^2(u) - (R(u) - h(u))^2\right) \cdot \pi \cdot L_0 \cdot (1+u) \geq \left(R_0^2 - (R_0 - h_0)^2\right) \cdot \pi \cdot L_0 \quad (19)$$

$$\left(2R(u) \cdot h(u) - h^2(u)\right) \cdot (1+u) \geq (2R_0 - h_0) \cdot h_0 \quad (20)$$

and transforming and dividing with R_0^2:

$$\left(2\frac{R(u)}{R_0} - \frac{h(u)}{R_0}\right) \cdot \frac{h(u)}{R_0} \geq \frac{\left(2 - \frac{h_0}{R_0}\right) \cdot \frac{h_0}{R_0}}{1+u} \quad (21)$$

$$\left(\rho(u) - \frac{\Phi_0}{2} \cdot \delta(u)\right) \cdot \Phi_0 \cdot \delta(u) \geq \frac{2-\Phi_0}{1+u} \cdot \Phi_0 \quad (22)$$

$$\left(\rho(u) - \frac{\Phi_0}{2} \cdot \delta(u)\right) \cdot \delta(u) \geq \frac{1}{2} \cdot \frac{2-\Phi_0}{1+u}. \quad (23)$$

Obviously

$$0 < \Phi_0 \leq 1, \quad (24)$$

$$0 < \rho(u) \leq 1, \quad (25)$$

$$0 < \delta(u) \leq 1. \quad (26)$$

In *Eq.* (23) the equality means constant volume. $\rho(u)$ and $\delta(u)$ are monotonously decreasing functions ($0 \leq u < \infty$).

When solid rod is stretched $h_0 = R_0$, $\Phi_0=1$, $\rho(u)=\delta(u)$, hence *Eq.* (23) takes the following form:

$$\left(\rho(u) - \frac{1}{2} \cdot \rho(u)\right) \cdot \rho(u) \geq \frac{1}{2} \cdot \frac{1}{1+u} \quad (27)$$

$$\delta(u) = \rho(u) \geq \frac{1}{\sqrt{1+u}}. \quad (28)$$

Eq. (28), the right side limit function is generalized e.g. with choice:

$$\delta(u) = \rho(u) \geq \frac{1}{(1+u)^a} \geq \frac{1}{\sqrt{1+u}};\ 0 < a \leq \frac{1}{2}. \quad (29)$$

Similar process can be carried out for hollow rods (tubes) as well. Although $\delta(u) \neq \rho(u)$ in that case, hence only one of them can be chosen in the way described above. In case of the other quantity, conditions *Eq.* (17) and *Eq.* (23) should also be considered.

Let accordingly be (for the simpler conditions)

$$\delta(u) = \frac{1}{(1+u)^a}, \tag{30}$$

where $a > 0$.

If *Eq.* (30) is substituted into *Eqs* (17) and (23), the following results are obtained

$$1 \geq \rho(u) \geq \frac{\Phi_0}{2} \cdot \frac{1}{(1+u)^a} + \left(1 - \frac{\Phi_0}{2}\right) \cdot \sqrt{1 - \frac{(1+u)^2 - 1}{4\pi^2 \cdot k_0^2}}, \tag{31}$$

and

$$1 \geq \rho(u) \geq \frac{\Phi_0}{2} \cdot \frac{1}{(1+u)^a} + \frac{2-\Phi_0}{2} \cdot \frac{1}{(1+u)^{1-a}}. \tag{32}$$

If $a > 1$, the second block of *Eq.* (32) tends to infinity if $u \to \infty$ which contradicts the $\rho(u) \leq 1$ condition, hence condition $0 < a \leq 1$ must be fulfilled.

The right part of *Eq.* (32) can give an upper boundary function of the same form as (30) which is made stricter but also more simplified than *Eq.* (32):

$$\rho(u) \geq \rho_2(u) = \frac{1}{(1+u)^{b_2}}, \;\; b_2 = \min(a,\ 1-a), \tag{33}$$

since e.g. if $a < 1 - a$

$$\frac{\Phi_0}{2} \cdot \frac{1}{(1+u)^a} + \frac{2-\Phi_0}{2} \cdot \frac{1}{(1+u)^{1-a}} \leq \left(\frac{\Phi_0}{2} + \frac{2-\Phi_0}{2}\right) \cdot \frac{1}{(1+u)^a} = \frac{1}{(1+u)^a}. \tag{34}$$

Fig. 4 illustrates the expressions above. It is to be noted that *Eq.* (34) can be made more accurate, obviously. Similarly to *Eq.* (34), a boundary function or a simpler

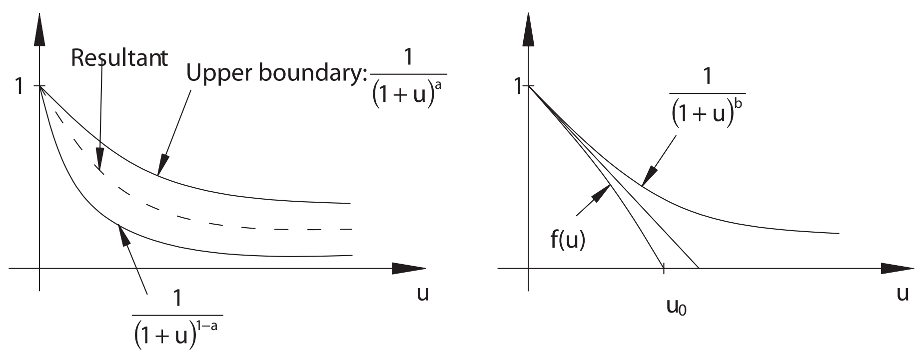

Fig. 4. Explanation of the boundary functions

condition that can be used more easily is looked for. For this purpose, the second term in *Eq.* (34) is examined.

Studying function *Eq.* (35) and its derivative *Eq.* (36)

$$f\,(u) = \sqrt{1 - \frac{(1+u)^2 - 1}{4\pi^2 \cdot k_0^2}};\ \ f\,(0) = 1, \tag{35}$$

$$\frac{d}{du} f\,(u) = \frac{1}{2 \cdot \sqrt{1 - \frac{(1+u)^2 - 1}{4\pi^2 \cdot k_0^2}}} \cdot \left(-\frac{2 \cdot (1+u)}{4\pi^2 \cdot k_0^2} \right) < 0. \tag{36}$$

It can be seen from *Eq.* (36) that function $f\,(u)$ is monotonously decreasing *Fig. (2 b)*, moreover the derivative is concave downward. Let be $f\,(u) = 0$, i.e.

$$u_0 :\ 1 = \frac{(1+u_0)^2 - 1}{4\pi^2 \cdot k_0^2} \ \Rightarrow\ u_0 = \sqrt{1 + T_0^2} - 1, \tag{37}$$

where

$$T_0^2 = 4\pi^2 \cdot k_0^2. \tag{38}$$

Accordingly

$$f\,(u) \le \frac{1}{(1+u)^b} = g\,(u)\,, \tag{39}$$

if

$$\left.\frac{d}{du} f\,(u)\right|_{u=0} \le \left.\frac{d}{du} g\,(u)\right|_{u=0}, \tag{40}$$

where

$$\frac{d}{du} g\,(u) = -\frac{b}{(1+u)^{1+b}}. \tag{41}$$

$$\left.\frac{d}{du} f\,(u)\right|_{u=0} = -\frac{1}{2} \cdot \frac{2}{4\pi^2 \cdot k_0^2} = -\frac{1}{T_0^2} \le -b = \left.\frac{d}{du} g\,(u)\right|_{u=0}, \tag{42}$$

i.e.

$$\frac{1}{T_0^2} \ge b \ \Leftrightarrow\ \left.\frac{d}{du} f\,(u)\right|_{u=0} \le \left.\frac{d}{du} g\,(u)\right|_{u=0}. \tag{43}$$

Consequently

$$\frac{\Phi_0}{2} \cdot \frac{1}{(1+u)^a} + \left(1 - \frac{\Phi_0}{2}\right) \cdot \sqrt{1 - \frac{(1+u)^2 - 1}{4\pi^2 \cdot k_0^2}} \le \frac{\Phi_0}{2} \cdot \frac{1}{(1+u)^a} + \frac{1 - \frac{\Phi_0}{2}}{(1+u)^{\frac{1}{T_0^2}}} \le$$

$$\le \frac{\Phi_0}{2} \cdot \frac{1}{(1+u)^a} + \frac{1 - \frac{\Phi_0}{2}}{(1+u)^{b_1}} = \frac{1}{(1+u)^{b_1}}, \tag{44}$$

where

$$b_1 = \min\left(a,\ \frac{1}{T_0^2}\right) \tag{45}$$

Thus

$$1 \geq \rho\,(u) \geq \rho_1\,(u) = \frac{1}{(1+u)^{b_1}}. \tag{46}$$

Finally a simple, applicable (while constrictable) condition is obtained for *ρ(u)* as *Eqs* (33) and (46) are connected:

$$1 \geq \rho\,(u) \geq \max\left(\rho_1\,(u)\,,\ \rho_2\,(u)\right) = \max\left(\frac{1}{(1+u)^{b_1}},\ \frac{1}{(1+u)^{b_2}}\right) = \frac{1}{(1+u)^{b}}, \tag{47}$$

i.e.

$$1 \geq \rho\,(u) \geq \frac{1}{(1+u)^{b}}, \text{ where} \quad b = \min\left(a,\ 1-a,\ \frac{1}{T_0^2}\right) \tag{48}$$

If $\rho\,(u) \geq \frac{1}{(1+u)^{b}}$, conditions (17) and (23) are fulfilled and that is equivalent to

$$\rho(u) = \frac{1}{(1+u)^{c}} \geq \frac{1}{(1+u)^{b}}, \tag{49}$$

where

$$0 < c \leq b = \min\left(a,\ 1-a,\ \frac{1}{T_0^2}\right). \tag{50}$$

This result *Eq.* (49) will be used in further development to determine the tensile properties of braided fiber reinforced composite tubes.

2. Experimental Materials

Epoxy-acrylate (vinylester) resins from DOW Chem. Co.: DERAKANE D 411 has been used in our experiments which is crosslinkable by electron beam without any addition.

The Tenax® STS 5631 carbon fiber rovings that contained 24,000 elementary fibers were used in our experimental work. The STS type rovings are a special type suitable for modern industrial application as well as braiding. The fibers were sized by ca. 1% polyurethane. *Table 1* shows the properties of applied carbon fibers.

Muratec J32 horizontal braiding machine made by Muratec Ltd., Kyoto, Japan which was set up in the Institute for Composite Materials at the University of Kaiserslautern, Germany was used to fabricate the circle profiles. It had 32 carriers and 16 laid-in and arbitrary stuffer roving inputs. The bobbin and pulling speed could be modified.

For the high energy electron beam curing a LUE-8 type electron accelerator was chosen, operating at 8 MeV and 650 μA electron-current, at FE-MA Co. Budapest, Hungary. The applied dose was 172 kGy.

The contraction parameter for applied fiber bundle cell model was determined by Messphysik Videoextensometer ME-46 made by Messphysik Materials Testing

Table 1. Properties of Tenax® STS 5631 roving

Property	Tenax® STS 5631
Tensile strength of a fiber [MPa]	4,000
Tensile modulus of a fiber [GPa]	240
Density of a fiber [g/cm^3]	1.77
Fiber diameter [μm]	7
Number of elementary fibers	24,000

GmbH, Austria on which simultaneous non-contacting measurement of both longitudinal and lateral strain could be performed.

3. Experimental Results

In *Fig. 5* the neck-forming of braided composite can be seen. *Fig. 6* shows the ratio of external radii as a function of the longitudinal strain. It can be seen clearly that the modelled contraction function using *Eq.* (49) estimates well the real ratio of external radii up to neck-forming.

4. Conclusion

It can be seen clearly that the model described the external radii of braided composite well. This result will be used in our further development to determine the tensile properties of that composite.

Acknowledgement

The authors would like to express their thanks to Tenax Ltd. for supplying the carbon fiber rovings, to Budaplast Rt. for providing us with the vinylester resin suitable for electron treatment; to FE-MA Kft. Hungary, who let us use the LUE 8 type electron accelerator; to IVW Universität Kaiserslautern, Germany where we braided, to Hodács Kft. where we impregnated the braids, to National Scientific Research Fund of Hungary for supporting the project reported through grants OTKA T 038220 and OTKA T 037733, to the Cleveland Hungarian Development Panel and Hungarian Academy of Engineering –Králik Fund for financial support.

Fig. 5. Neck-forming of tensile-loaded markered braided composite

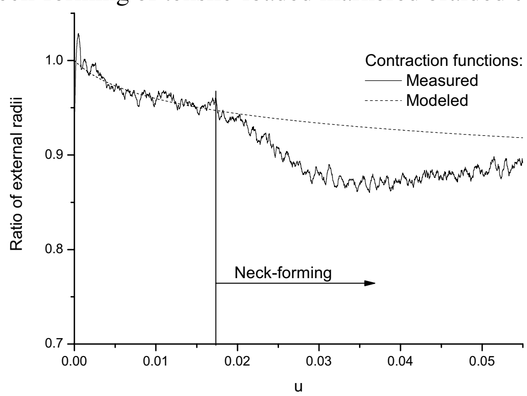

Fig. 6. The measured and the modelled contraction functions (number of bobbins: 16, fiber content: 0.23; braiding angle: 61°)

References

[1] PHOENIX, S. L., Mechanical Response of a Tubular Braided Cable with an Elastic Core, *Textile Research Journal*, **48**, 1978, pp. 81–91.

[2] VAS, L. M., A statisztikus kötegszilárdság és alkalmazása a szál- és fonalvizsgálatokban (The Statistical Fiber Bundle Strength and its Application in Testing Fibers and Yarns), *Magyar Textiltechnika* (Hungarian Textile Technique), **43**, 1990, pp. 165–185.

[3] VAS, L. M., Újabb eredmények a síkban rendezett szál- és fonalkötegek szakítási elméletében (Latest Results in the Tensile Test Theory of Fiber and Yarn Bundles Ordered into Plane), *Magyar Textiltechnika* (Hungarian Textile Technique), **45**, 1992, pp. 71–75, 137–142, 187–191.

[4] VAS, L. M. – CSÁSZI, F., Use of Composite-Bundle Theory to Predict Tensile Properties of Yarns, *Journal of the Textile Institute*, **84**, 1993, pp. 448–463.

[5] VAS, L. M. – HALÁSZ, G., Modelling the Breaking Process of Twisted Fiber Bundles and Yarns, *Periodica Polytechnica, Ser. Mech. Eng.* **38**, 1994, pp. 325–350.

[6] VAS, L. M. – RÁCZ, ZS., Modelling and Testing The Fracture Process of Impregnated Carbon Fiber Roving Specimens During Bending – Part I: Fiber Bundle Model, *Journal of Composite Materials*, **38**, 2004, pp. 1757–1786.

[7] VAS, L. M. – RÁCZ, ZS.– NAGY, P., Modelling and Testing The Fracture Process of Impregnated Carbon Fiber Roving Specimens During Bending – Part II: Experimental Studies, *Journal of Composite Materials*, **38**, 2004, pp. 1787–1802.